will further add to the activation barrier. The transition-state structure for the addition of CH_4 to $Ru(CO)_4$ is given in Figure 7e. Note the modest elongation of the C-H bond, $R(H-CH_3)$ = 1.17 Å, as a result of the weak interaction in **9d**. The low energy of the $1b_2$ orbital (**5d**) on $M(CO)_4$ is also contributing to the fact that $M(CO)_4(H)(CH_3)$ is less stable than $Cp(L)(H)(CH_3)$.

The calculated $M-CH_3$ bond energies are given in Table II. The strength of the $M-CH_3$ bonds follows the order $D(Ir-CH_3) > D(Rh-CH_3) > D(Os-CH_3) > D(Ru-CH_3)$. This order is determined by the same factors as the analogous order for the corresponding M-H bonds; see section IV and Table II. The $M-CH_3$ linkages are consistently weaker than the corresponding M-H bonds by 60-100 kJ mol^{-1}. This differential, which is characteristic for late-transition metals, has been rationalized in a previous study.[12] The calculated $Ir-CH_3$ bond strength of 260 kJ in $Cp(PH_3)Ir(H)(CH_3)$ is in line with the experimental value of 235 kJ mol^{-1} obtained by Stoutland[1] et al. in $(C_5Me_5)(PMe_3)Ir(CH_3)_2$. It is exceptionally high, attesting to the unique features of the Cp(L)Ir system discussed above. Other $Ir-CH_3$ bonds are much weaker. Thus, $D(Ir-CH_3)$ in $(PMe_3)_2(CO)Ir(I)(Cl)(CH_3$ is measured[1] to be 148 kJ mol^{-1}, which is comparable to our calculated $D(Os-CH_3)$ value of 182 kJ mol^{-1} in the isoelectronic $Os(CO)_4(H)(CH_3)$ system. In both systems the $M-CH_3$ linkage is destabilized by the interaction of a fully occupied d-based orbital, **2c**.

VI. Concluding Remarks

We have, in the present study, investigated the molecular and electronic structures of the coordinatively unsaturated d^8 fragments Cp(L)M and $M(CO)_4$, as well as their potentials as catalysts in the functionalization of CH_4 according to Scheme I. We have found that the Cp(L)M fragments are unique as C-H activating agents, step b of Scheme I, in that they only have empty d-based orbitals interacting with the incoming C-H bond. Most other mononuclear d^8 systems, including the $M(CO)_4$ systems, have empty as well as occupied metal-based orbitals, and the latter will impede the addition reaction in step b. Further, the fact that the 2a″ HOMO (**2e**) has a relatively high energy helps reduce the energy barrier for the addition of H-H and $H-CH_3$ bonds. The high energy of 2a″ is further instrumental in stabilizing the products from the oxidative addition reactions. The generation of the active species Cp(L)M, step a of Scheme I, from the coordinatively saturated Cp(L)MZ system was investigated in some detail for Z = CO, PH_3, and H_2. It was concluded that too much energy, in the order of 200 kJ mol^{-1}, is required for step a with Z = CO. The step is more favorable for $Z = H_2$ and in particular $Z = PH_3$. We have assumed that the C-H bond in CH_4 is activated by a 16-electron species. Marx[43] and Lees have recently suggested that $CpIr(CO)_2$ might activate CH_4 by an associative mechanism without prior loss of CO. The mechanism suggested by Marx and Lees has not been investigated in the present study.

Acknowledgment. This investigation was supported by the Natural Sciences and Engineering Research Council of Canada (NSERC). We thank Professor E. J. Baerends and Professor W. Ravenek for a copy of their vectorized LCAO-HFS program system and the University of Calgary for access to their Cyber-205 facility.

Registry No. $Cp(CO)Rh(H)_2$, 122699-95-0; $Cp(PH_3)Rh(H)_2$, 122699-96-1; $Cp(CO)Ir(H)_2$, 78829-47-7; $Cp(PH_3)Ir(H)_2$, 87966-29-8; *cis*-$Ru(CO)_4(H)_2$, 21029-23-2; *cis*-$Os(CO)_4(H)_2$, 18972-42-4; $Cp(CO)Rh(H)(CH_3)$, 108582-17-8; $Cp(PH_3)Rh(H)(CH_3)$, 122699-97-2; $Cp(CO)Ir(H)(CH_3)$, 87739-22-8; $Cp(PH_3)Ir(H)(CH_3)$, 122699-98-3; *cis*-$Ru(CO)_4(H)(CH_3)$, 122699-99-4; *cis*-$Os(CO)_4(H)(CH_3)$, 22639-03-8; Cp(CO)Rh, 86803-04-5; $Cp(PH_3)Rh$, 86803-01-2; Cp(CO)Ir, 87966-32-3; $Cp(PH_3)Ir$, 87966-30-1; $Ru(CO)_4$, 29718-13-6; $Os(CO)_4$, 27857-69-8; $Cp(CO)_2Rh$, 12192-97-1; $Cp(PH_3)(CO)Rh$, 122700-00-9; $Cp(CO)_2Ir$, 12192-96-0; $Cp(PH_3)_2Rh$, 122700-01-0; $Cp(PH_3)(CO)Ir$, 122700-02-1; $Cp(PH_3)_2Ir$, 122700-03-2.

(43) Marx, D. E.; Lees, A. L. *Inorg. Chem.* **1988**, *27*, 1121.

Electrochemistry of Cytochrome *c*, Plastocyanin, and Ferredoxin at Edge- and Basal-Plane Graphite Electrodes Interpreted via a Model Based on Electron Transfer at Electroactive Sites of Microscopic Dimensions in Size

Fraser A. Armstrong, Alan M. Bond,[1] H. Allen O. Hill,* B. Nigel Oliver, and Ioanna S. M. Psalti

Contribution from the Inorganic Chemistry Laboratory and the Oxford Centre for Molecular Sciences, South Parks Road, Oxford, OX1 3QR, Great Britain. *Received November 30, 1988*

Abstract: The electrochemistry of a range of electron-transfer proteins at edge- and basal-plane graphite electrodes has been reconsidered using a *microscopic* model, which involves fast electron transfer at very small oxygen-containing electroactive surface sites. This model assumes that mass transport to the electrode occurs by radial diffusion when the density of the surface active sites is low (as is generally true in the case of the basal-plane graphite electrode) and by linear diffusion when the density of the active sites is increased sufficiently to cause overlap of the diffusion layers. With this model it is now proposed that the electrochemistry of cytochrome *c*, plastocyanin, and ferredoxin occurs with a very fast rate of charge transfer ($\geq$1 cm s^{-1}) at both edge- and basal-plane graphite electrodes. Critical factors, such as the mode of surface preparation (including covalent derivatization), the pH, and the presence in the electrolyte of cations such as Mg^{2+} or $Cr(NH_3)_6^{3+}$, control the *density* of surface sites, which result in the electrochemistry of a specific protein. This contrasts with the conclusion that has been reached previously based upon a conventional macroscopic model, which supposes that the *rate* of electron transfer is subject to enhancement or depression through these factors. The proposal that the electron-transfer process at the protein-graphite electrode interface is very fast over a wide range of conditions is now consistent with homogeneous kinetic studies where electron-transfer reactions of proteins, particularly amongst physiological partners, are also known to be fast.

Chemical and electrochemical studies of redox proteins have attracted considerable attention over the last few years.[2-5] Generally, homogeneous rates of electron transfer have been found to be fast. In contrast, heterogeneous rates of electron transfer

0002-7863/89/1511-9185$01.50/0

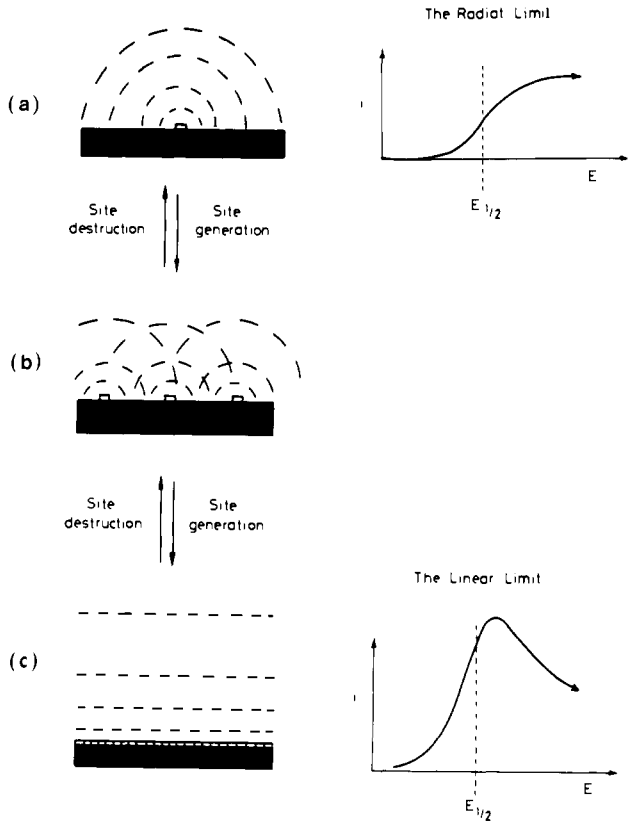

Figure 1. Schematic representation of the conversion of radial to linear diffusion, as the density of specific electroactive surface sites increases.

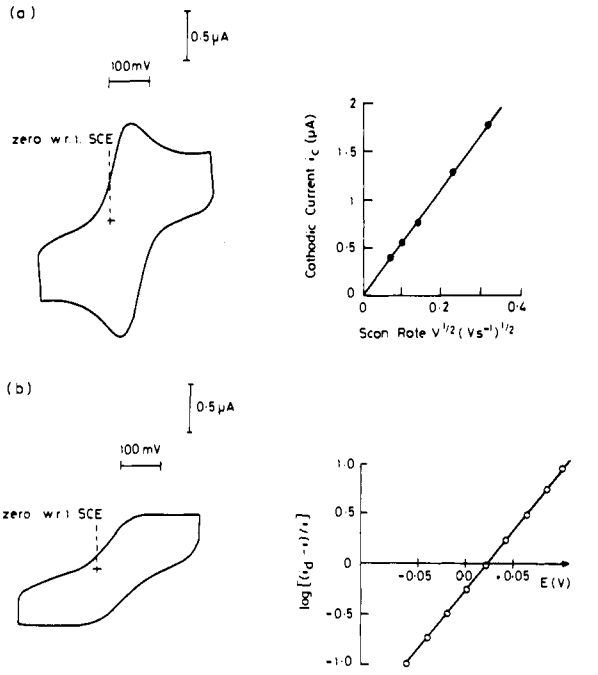

Figure 2. Cyclic voltammograms for reduction of 150 μM cytochrome *c* in a 5 mM Tricine buffer (pH 8.0) containing 100 mM NaCl at (a) polished PGE and (b) freshly cleaved PGB electrodes. Scan rate, 20 mV s^{-1}; temperature, 20 °C. Also shown are a plot of peak current for the reduction process at the edge-plane electrode vs the square-root of the scan rate, $\nu^{1/2}$, verifying the predominance of linear diffusion for (a) and a plot of log $[(i_d - i)/i]$ vs the potential E at the basal-plane electrode verifying the predominance of radial diffusion for (b).

at electrode surfaces have been reported to range from so slow or irreversible that no electrochemistry (voltammetry) is observed (e.g., at bare metal electrodes) to very fast (reversible) at some classes of chemically modified electrodes.[2-10]

The concept that the heterogeneous rate of electron transfer of proteins is critically dependent on the nature of the electrode surface has been widely accepted.[2-10] However, calculations of heterogeneous rates of electron transfer at different surfaces and related concepts of reversible, (fast rates), irreversible (slow rates), or quasi-reversible (intermediate rates) electrochemistry (voltammetry) have been based on a macroscopic model of electron transfer, which assumes that mass transport occurs via linear diffusion to an electrode having a large electroactive surface area relative to the size of the protein. We report herein that the validity of this model must be reassessed to consider the situation in which the electroactive sites are of *microscopic* rather than macroscopic dimensions.[11,12]

The relevant theory is summarized in Figure 1. At an isolated single site of microscopic dimensions, mass transport is radial and the shape of the associated current–voltage curve is sigmoidal. As further active sites are generated, the diffusion layers overlap, eventually producing the familiar, limiting situation of linear diffusion. Figure 2 shows a comparison of voltammograms for cytochrome *c* at freshly cleaved basal-plane and polished edge-plane graphite electrodes. Using the macroscopic model and theory based on linear diffusion, the rate of electron transfer calculated from the peak shaped curve at the edge plane (Figure 2a) is deduced to be fast (close to reversible), while the drawn-out curve observed at the basal-plane electrode (Figure 2b) corresponds to a much slower rate of electron transfer.[10] An intermediate rate of electron transfer is calculated from data obtained at a polished basal-plane electrode. However, if a *microscopic* rather than macroscopic model of electron transfer is employed, as illustrated in Figure 1, in which it is assumed that electron transfer takes place *only* at specific areas (functionalized sites) of microscopic dimensions, then calculations[11] are consistent with reversible electrochemistry for cytochrome *c* at edge- and basal-plane and polished basal-plane graphite electrodes with a heterogeneous rate constant for charge transfer that always exceeds 1 cm s^{-1}. The new model assumes that electron transfer occurs at arrays of oxygen-containing functionalized electroactive sites, which are of microscopic dimensions in size, and that *no* electron transfer occurs at a bare nonfunctionalized carbon electrode. Oxygen-containing sites are generated by surface abrasion (polishing), and

(1) On leave of absence from the Division of Chemical and Physical Sciences, Deakin University, Geelong 3217, Victoria, Australia.

(2) Frew, J. E.; Hill, H. A. O. *Eur. J. Biochem.* **1988**, *172*, 261–269.

(3) Armstrong, F. A.; Hill, H. A. O.; Walton, N. J. *Acc. Chem. Res.* **1988**, *21*, 407–413.

(4) Armstrong, F. A.; Hill, H. A. O.; Walton, N. J. *Q. Rev. Biophys.* **1986**, *18*, 261–322.

(5) Hill, H. A. O. *Pure Appl. Chem.* **1987**, *59*, 743–748.

(6) Fan, K. J.; Alcutsu, H.; Niki, K. *Denki Kagaku* **1987**, *55*, 664–668.

(7) Heineman, W. R.; Norris, B. J.; Goelz, J. F. *Anal. Chem.* **1975**, *47*, 79–84.

(8) Kono, T.; Nakamura, S. *Bull. Agric. Chem. Soc. Jpn.* **1958**, *22*, 399–406.

(9) Albery, W. J.; Eddowes, M. J.; Hill, H. A. O.; Hillman, A. R. *J. Am. Chem. Soc.* **1981**, *103*, 3904–3910.

(10) Armstrong, F. A.; Cox, P. A.; Hill, H. A. O.; Lowe, V. J.; Oliver, B. N. *J. Electroanal. Chem.* **1987**, *217*, 331–366.

(11) Armstrong, F. A.; Bond, A. M.; Hill, H. A. O.; Psalti, I. S. M.; Zoski, C. G. *J. Phys. Chem.* **1989**, *93*, 6485–6493.

(12) It has been recognized in the past that *macroscopic* inhomogeneity of the electrode surfaces gives rise to effects associated with nonlinear diffusion: Gueshi, T.; Koichi, T.; Matsuda, H. *J. Electroanal. Chem.* **1978**, *89*, 247–260; **1979**, *101*, 29–38. Microstructures on electrodes comprised of adsorbed polymer chains (Amatore, C.; Savéant, J. M.; Tessier, D. *J. Electroanal. Chem.* **1983**, *147*, 39–51) or highly oriented organic monomolecular layers (Sabatani, E.; Rubinstein, I. *J. Phys. Chem.* **1987**, *91*, 6663–6669) produce *microscopic* inhomogeneity of the surface. These authors have related the diffusion mechanics to the size of the active sites and the distance separating them. These models are unsuited for the case of "natural" array electrodes (oxygen-functionalised carbon surfaces) since the size of the active areas is not known and unlikely to be uniform.

the surface density of such functionalized sites at freshly cleaved basal-plane electrodes is very low. Under these conditions, radial diffusion terms are dominant (Figure 1a) and sigmoidal-shaped voltammograms result. At a polished edge-plane electrode, extensive functionalization of the surface is favored so the density of active sites increases to the point where diffusion layers overlap (Figure 1b), destroying radial diffusion and leaving the linear diffusion terms as the dominant ones (Figure 1c). The polished basal-plane electrode has an intermediate surface density of electroactive sites. That is, the different wave forms in Figure 2 are simply a result of an extremely fast rate of electron transfer taking place at electrodes of variable active-site density and are *not* related to variable rates of electron transfer.

The concept of an extremely fast electron-transfer rate at functionalized graphite electrode surfaces is intrinsically satisfying because homogeneous rates of electron transfer for chemical reactions involving redox proteins are known to be fast, particularly among physiological partners. In this paper, the present model of electron transfer to oxygen-functionalized electroactive sites is applied generally to the electrochemistry of cytochrome *c*, plastocyanin, and ferredoxin at various types of graphite electrodes and compared with conclusions based on the macroscopic model.

Experimental Section

Most of the experimental procedures relating to the purification of proteins and chemical reagents, and the preparation of edge- and basal-plane graphite electrodes used in this work have been described elsewhere.[10] A brief description only of important aspects of the experimental details is therefore provided in this paper. Horse heart cytochrome *c* (Sigma type VI) was purified by the method of Brautigan et al.[13] Plastocyanin and [2Fe–2S] ferredoxin were isolated from spinach using a modification of the procedure of Borchert and Wessels.[14a] Rubredoxin and the 2[4Fe–4S] ferredoxin from *Clostridium pasteurianum* were obtained by the use of published procedures.[14b] All proteins were stored in the pure state as desalted frozen droplets in liquid nitrogen. The following buffers were used: *N*-(2-hydroxyethyl)piperazine-*N*′-2-ethanesulfonic acid, HEPES; *N*-[2-(hydroxymethyl)-1,1-bis(hydroxymethyl)ethyl]glycine, Tricine; sodium acetate. The pH was measured with a standard glass electrode and a pH meter.

Disks of pyrolytic graphite (Le Carbone, Portslade, Sussex) were machined and oriented with the disk face parallel to the basal (PGB) or edge (PGE) plane. The electrodes made in this way were housed in Teflon sheaths, and internal electrical connection was made via a brass rod. The sides of the electrode were sealed with epoxy resin. Polishing was carried out manually, with an aqueous slurry of 0.3-μm alumina or with a 0.25-μm diamond powder slurry, followed by sonication. Exposure of a fresh surface of basal-plane electrode was carried out by slicing with a clean razor blade. All experiments were conducted using an oxygen-free argon atmosphere. Cyclic voltammetric experiments were performed with an Ursar Scientific potentiostat and scan unit using a standard three-electrode cell arrangement consisting of an edge-plane or basal-plane graphite electrode, saturated calomel reference electrode (E = +244 mV vs SHE at 25 °C) and a platinum auxiliary electrode.

Results and Discussion

(a) Cytochrome *c*. Data obtained from X-ray photoelectron spectroscopy[10] and other studies[15] have established the presence of C–O functional groups on the graphite surface: carbonyl, phenolic, carboxylic, and ether-like groups are all thought to be present. At the basal-plane electrode, the carbon-to-oxygen ratio at the surface is very low (O/C = 0.02). On polishing, this increases to 0.11, and, with an edge plane, the ratio may be as high as 0.33. The surface density of active sites and the shape of the cyclic voltammograms are therefore a function of the method of fabrication and history of the electrode.[10] Thus, the observation of an almost sigmoidal-shaped curve for cytochrome *c* at a basal-plane electrode (Figure 2b) with a half-wave potential, $E_{1/2}$, equal to the standard redox potential, $E°$ (with an associated error of ±5 mV), and a linear plot of E vs log $(i_d - i)/i$, (E = potential, i = current, i_d = limiting current) with a slope of $2.303RT/F$ (±0.002 V) over the temperature range 15–25 °C, is consistent with a reversible process at an array of microscopically small and well-spaced electroactive sites.[11] In contrast, the peak-shaped response at the edge plane (Figure 2a), with the average of the reduction and oxidation peak potentials giving an $E°$ value equal to the value obtained at $E_{1/2}$ for the basal-plane electrode (within the experimental error of ±5 mV), is also consistent with a reversible process but under conditions where the diffusion layers overlap and destroy radial diffusion.[11] The polished basal-plane electrode represents an intermediate case of behavior, but the electron-transfer process is always reversible.[11] Various aspects of the theory where radial diffusion dominates (the steady state) are available in the literature.[11,16-18] The linear diffusion case also has been well documented in numerous books and reviews[19] since the pioneering work by Nicholson.[20] The important point to note is that, according to the microscopic model, the change in shape is *not* a reflection of the change of rate of electron transfer. In contrast, it is the use of the peak-to-peak separation and the Nicholson criteria,[20] in conjunction with a macroscopic model of electron transfer, which has led to the conclusion that reduction of cytochrome *c* at the basal plane is much slower than at the edge-plane graphite electrode.

To test further the microscopic model, as applied to cytochrome *c* and other proteins, the obvious experiments to undertake are surface modifications, which deliberately alter the density of electroactive sites at the electrode. Results for various systems are shown together in Figure 3. For cytochrome *c*, it has been proposed that positively charged groups around the active-site heme edge interact with deprotonated C–O functional groups at the electrode surface.[10] Thus, blocking agents, which can bind preferentially to the oxygen groups on the surface, decrease the surface density of suitable sites at which electron transfer to the protein can take place. Figure 3 (a and b) shows the influence on the electrochemistry of cytochrome *c* when triphenylsilane blocking groups are attached[21] to a carbon electrode via the process

$$\text{EC–OH} + \text{ClSiPh}_3 \rightarrow \text{EC–O–SiPh}_3 + \text{HCl} \qquad (1)$$

where EC–OH is the graphite electrode surface. According to the microscopic model, the almost sigmoidal (Figure 3a), rather than peak-shaped curves (Figure 3b), which are observed in the presence of silane blocking groups, are not the result of slow electron transfer as previously proposed.[21] Rather, a decrease in the number of active sites leads to a predominance of radial over linear diffusion but the *rate* of electron transfer remains extremely fast. At the silane-derivatized electrodes, the corresponding plot of E vs log $(i_d - i)/i$ is linear with a slope of $2.303(RT/F \pm 0.002$ V) at 20 °C, and $E_{1/2} = E°$ with an experimental error of ±5 mV. This result (not shown) is identical with the reduction of cytochrome *c* at a basal-plane electrode, when the surface density of active sites, which in this case are effectively present as electrode imperfections, is also lower than at the edge-plane electrodes (see Figure 2). The situation may be reversed; i.e., removal of the silyl groups by dissolution in methanolic KOH restores voltammetry similar to that of Figure 3b.

(13) Brautigan, D. L.; Ferguson-Miller, S.; Margoliash, E. *Methods Enzymol.* **1978**, *73*, 128.
(14) (a) Borchert, M. T.; Wessels, J. S. C. *Biochim. Biophys. Acta* **1970**, *197*, 78–86. (b) Thomson, C. L.; Johnson, C. E.; Dickson, D. P. E.; Cammack, R.; Hall, D. O.; Weser, U.; Rao, K. K. *Biochem. J.* **1974**, *139*, 97–103.
(15) See, for example: (a) Kamau, G. N.; Willis, W. S.; Rusling, J. F. *Anal. Chem.* **1985**, *57*, 545–551. (b) Schlögl, R.; Boehm, H. P. *Carbon* **1983**, *21*, 345–358. (c) Proctor, A.; Sherwood, P. M. A. *Carbon* **1983**, *21*, 53–59. (d) Takahagi, T.; Ishitani, A. *Carbon* **1984**, *22*, 43–46. (e) Engstrom, R. C.; Strasser, V. A. *Anal. Chem.* **1984**, *56*, 136–141. (f) Cabaniss, G. E.; Diamantis, A. A.; Murphy, W. R.; Linton, R. W.; Meyer, T. J. *J. Am. Chem. Soc.* **1985**, *107*, 1845–1853.
(16) Bond, A. M.; Oldham, K. B.; Zoski, C. G. *J. Electroanal. Chem.* **1988**, *245*, 71–104.
(17) Bond, A. M.; Oldham, K. B.; Zoski, C. G. *Anal. Chim. Acta*, in press, in references therein.
(18) Zoski, C. G.; Bond, A. M.; Colyer, C. L.; Myland, J. C.; Oldham, K. B. *J. Electroanal. Chem.*, in press.
(19) See, for example: (a) Bard, A. J.; Faulker, L. R. *Electrochemical Methods*; John Wiley: New York, 1980. (b) Greel, R.; Peat, R.; Peter, L. M.; Pletcher, D.; Robinson, J. *Instrumental Methods in Electrochemistry*; Ellis Horwood: Chichester, 1985.
(20) Nicholson, R. S. *Anal. Chem.* **1965**, *37*, 1351–1355.
(21) Armstrong, F. A.; Brown, K. J. *J. Electroanal. Chem.* **1987**, *219*, 319–325.

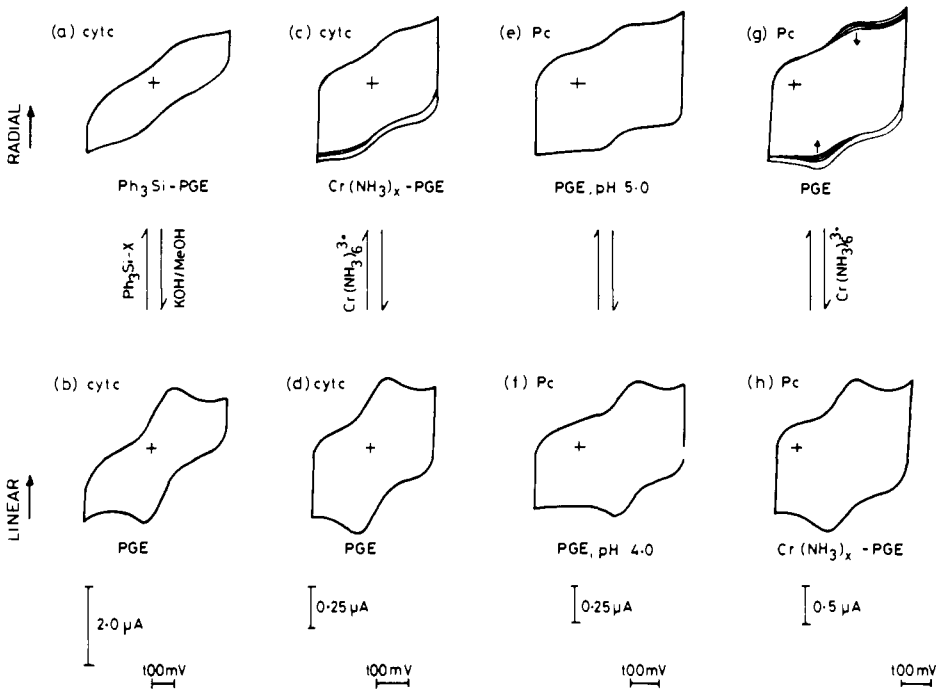

Figure 3. Modifications of the edge-plane graphite (PGE) electrode interface and their effect on the electrochemistry of: (a) 150 μM cytochrome *c* in 5 mM Tricine/100 mM NaCl buffer (pH 8.0 at Ph_3Si-modified PGE electrode; scan rate, 20 mV s^{-1}; temperature, 20 °C). (b) Same as in (a) at bare PGE electrode. (c) 50 μM cytochrome *c* in 5 mM Tricine/100 mM NaCl buffer (pH 8.0 at $Cr(NH_3)_x$-modified[22] PGE electrode; scan rate, 20 mV s^{-1}; temperature, 25 °C). (d) Same as in (c) at bare PGE electrode. (e) 25 μM plastocyanin in 5 mM acetate/1 mM KCl buffer (pH 5.0 at bare PGE electrode; scan rate, 20 mV s^{-1}; temperature, 3 °C). (f) Same as in (e) at pH 4.0. (g) 30 μM plastocyanin in 5 mM HEPES/100 mM KCl buffer (pH 7.0 at bare PGE electrode; scan rate, 20 mV s^{-1}; temperature, 20 °C). (h) Same as in (g) at $Cr(NH_3)_x$-modified PGE electrode.

Armstrong et al. have also shown[22] that it is possible to attach chromium(III) complexes to the C–O functional groups at an edge-plane graphite electrode. Reductive cycling of an ammoniacal solution of $Cr(NH_3)_6^{3+}$ produces surface complexes of the kind

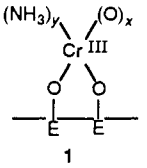

1

Figure 3 (c and d) shows the cyclic voltammograms for cytochrome *c* in the presence and absence of positively charged surface complexes. As in the previous case, a fully reversible steady-state sigmoidal-shaped response (Figure 3c) corresponding to reversible charge transfer at a low density of microscopic electroactive sites is transformed into the peak-shaped voltammogram (Figure 3d) in the absence of modification. Cytochrome *c* is a positively charged protein, and addition of groups of the same charge to the electrode surface has the effect of decreasing the surface density of electroactive sites. The addition to the solution of Mg^{2+} or $Pt(NH_3)_6^{4+}$ also causes a similar effect.

(b) Plastocyanin. The copper protein, plastocyanin, has an overall negative charge[23] at pH 7. It has been suggested that, at pH values less than about 5, considerable protonation of electrode surface functional groups takes place.[10,26] Thus, if electron transfer only occurs at these sites, the electrostatic binding interactions will be aided by low pH and the electrochemistry should appear to be pH-dependent, according to the microscopic model.

Figure 3 (e and f) shows the cyclic voltammetric response of plastocyanin as a function of pH at low ionic strength (<5 mM). The sigmoidal shape of the response at pH 5 (Figure 3e) can be attributed to a low concentration of well-separated microscopic sites for electron transfer. The peak-shaped response at pH 4 (Figure 3f) is associated with an increase in the density of these sites, giving rise to a predominance of linear over radial diffusion. Importantly, there is no evidence that electron transfer is slower at pH 5 nor that the change in pH alters the rate of electron transfer to less than the value consistent with a reversible process. That is, the electrochemistry of plastocyanin, as is the case with cytochrome *c*, is extremely site-specific. The fast electron transfer occurs at suitably functionalized interaction sites. It does not occur at all at deprotonated sites at which, presumably, the protein cannot be bound under the low ionic strength conditions.

Figure 3 (g and h) shows the response of plastocyanin in the absence and presence of the surface-attached chromium species (**1**) at an ionic strength of 0.1 M and pH 7.0. Under these conditions, considerable screening of electrostatic repulsion occurs and some sites are available on the unmodified electrode (Figure 3g). However, these are progressively destroyed, presumably by denaturation, coupled to irreversible adsorption. The situation is now reversed from that which pertains to cytochrome *c* [Figure 3 (c and d)]. The positively charged domains formed from $Cr(NH_3)_6^{3+}$ treatment of the electrode surface (**1**) promote reversible binding, and the electrochemistry is furthermore stable (Figure 3h). The population of suitable electrode sites is also modulated by the nature of the electrolyte, particularly the presence of multivalent cations.[10] This is seen clearly at pH values ≥6, i.e., conditions under which the electrode surface is deprotonated. Voltammograms measured[10] during the course of a titration of the electrochemistry of (for example) plastocyanin or ferredoxin by added $Cr(NH_3)_6^{3+}$ ions show analogous results, i.e., a progressive change from the radial-type case to one of linear diffusion.

(c) Ferredoxin. The ferredoxins, as is the case with plastocyanin, are negatively charged, and the shapes of cyclic voltammograms are varied by addition of multivalent cations. We have used the example of the electrochemistry of 2[4Fe-4S] ferredoxin from *C. pasteurianum* to demonstrate finally the variation of peak or plateau current with sweep rate, ν. Cytochrome *c* was not

(22) Armstrong, F. A.; Cox, P. A.; Hill, H. A. O.; Oliver, B. N.; Williams, A. A. *J. Chem. Soc., Chem. Commun.* **1985**, 1236–1237.
(23) Scawen, M. O.; Ramshaw, J. A. M.; Boulter, D. *Biochem. J.* **1975**, *147*, 343–349.
(24) Margoliash, E.; Schejter, A. *Adv. Protein Chem.* **1966**, *21*, 113–286.
(25) Katoh, S. In *Encylopaedia of Plant Physiology*; Pirson, A., Zimmerman, M. H., Eds.; John Wiley: New York, 1977; Vol. 5, pp 247–252.
(26) Deakin, M. R.; Stutts, K. J.; Wightman, R. M. *J. Electroanal. Chem.* **1985**, *182*, 113–122.

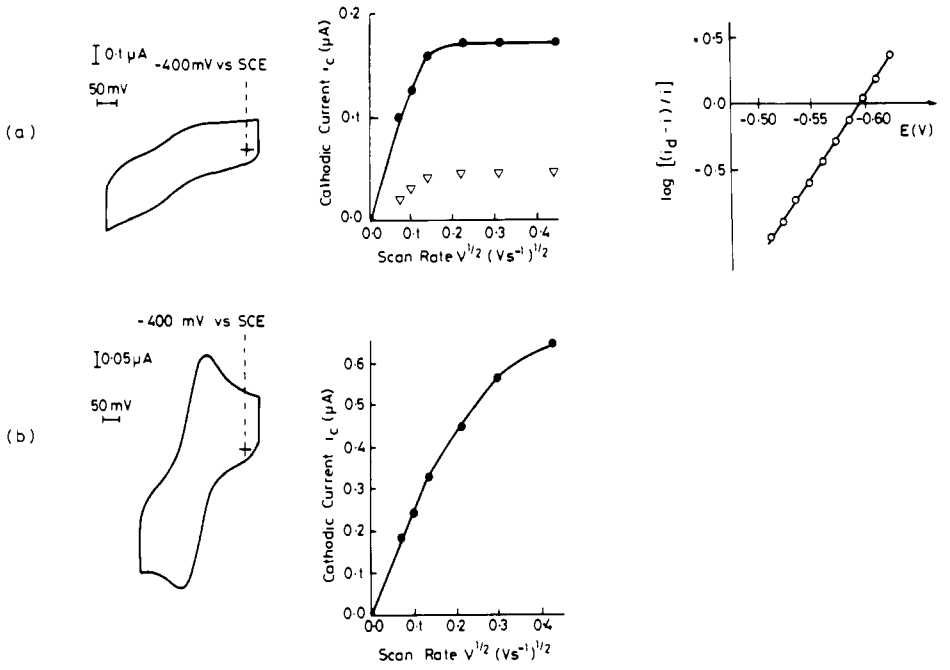

Figure 4. Cyclic voltammograms for 60 μM *Clostridium pasteurianum* 2[4Fe-4S] ferredoxin in 20 mM HEPES/100 mM NaCl buffer (pH 7.4, 6 mM $Cr(NH_3)_6^{3+}$; scan rate, 20 mV s^{-1}; temperature, 20 °C) at (a) freshly cleaved and (b) polished basal-plane electrode. Plots of cathodic current i_c vs scan rate $v^{1/2}$ (shown as ●) and, in the case of (a), anodic current vs $v^{1/2}$ (shown as ▽) and log $[(i_d - i)/i]$ vs the potential E (shown as ○) are also included.

appropriate for this due to interference, at high scan rates, by a surface peak in the background current at the basal-plane electrode. The electrochemistry of ferredoxin at freshly cleaved basal-plane graphite in the presence of $Cr(NH_3)_6^{3+}$ ions is reversible, as shown by the plot of log $[(i_d - i)/i]$ vs the potential, E (Figure 4a, ○). The form of the i_c vs $v^{1/2}$ plot is clearly sensitive to the density of surface active sites. For example,[10] at the polished edge electrode, i_c varies linearly with $v^{1/2}$ at least up to 200 mV s^{-1}. In the case of the polished basal-plane electrode (Figure 4b, ●), the linearity extends to 20 mV s^{-1}, thereafter curving off; while at the cleaved basal-plane electrode, the current (Figure 4a, ●) becomes *maximal* at 50 mV s^{-1}. The same trend is shown by the plot of the anodic current vs $v^{1/2}$ (Figure 4a, ▽). The estimated anodic current appears lower than the estimated cathodic current due to extrapolation from the unsymmetrical background.

Conclusion

A microscopic model for the electron transfer at the protein–electrode interface (which occurs reversibly at active sites of microscopic dimensions in size) now rationalizes many observations reported for redox protein electrochemistry at graphite electrodes. The macroscopic model previously used to describe results required that the rate of electron transfer is enhanced or depressed by various factors. With the microscopic model, the concept of very rapid electron transfer at the electrode interface at *specific sites* seems consistent with expectations based on homogeneous redox processes involving biologically important proteins. Reactions of these are usually reported to be fast. For simple small molecules, such as ferrocene monocarboxylic acid, $Ru(NH_3)_6^{3+}$ and $Fe(CN)_6^{3-}$, silination of the electrode surface has little if any effect.[21] Electroactivity of these appears *nonselective* with respect to the nature of electrode domains. By contrast, the redox activity of proteins is *selective*. Electron transfer to and from the active site of the protein is anisotropic and might be addressed only when binding interactions assist attainment of the correct orientation for electron transfer.[27]

The conclusions in this study are likely to apply to other forms of carbon electrode[28-30] and other surfaces that may have microelectrode or array-like properties.[31-33] Many reports of electron-transfer rates for proteins at carbon electrodes[2-6,34] may therefore need to be reevaluated. The present work suggests that published heterogeneous charge-transfer rate constants will not be correct in circumstances where radial, rather than linear, diffusion is the important mode of mass transport to the electrode surface. Indeed even the mass-transport problems of electron-carrier proteins reacting at membrane sites of photooxidative or oxidative phosphorylation may be considered in terms of a microelectrode array.

Acknowledgment. We thank the SERC for support. F.A.A. thanks the Royal Society for a University Research Fellowship. A.M.B. thanks the University of Oxford for the hospitality extended during his leave and Deakin University for financial support making this possible.

Registry No. $Cr(NH_3)_6^{3+}$, 14695-96-6; $Pt(NH_3)_6^{4+}$, 18536-12-4; Mg, 7439-95-4; cytochrome *c*, 9007-43-6; graphite, 7782-42-5.

(27) Mayo, S. L.; Ellis, W. R. R., Jr.; Crutchley, R. J.; Gray, H. B. *Science* **1986**, *233*, 948.
(28) Lipkin, S. M.; Cahen, G. L.; Stoner, G. E.; Scriber, L. L.; Gileadi, E. *J. Electrochem. Soc.* **1988**, *135*, 368–372.
(29) Bowling, R.; Packard, R.; McCreery, R. L. *J. Electrochem. Soc.* **1988**, *135*, 1605–1606.
(30) Aoki, K.; Kaneko, H.; Nozaki, K. *J. Electroanal. Chem.* **1988**, *247*, 29–36.
(31) Di Marino, M.; Marassi, R.; Santucci, R.; Brunori, M.; Ascoli, F. *Biochem. Bioenerg.* **1987**, *17*, 27–34.
(32) Swiatkowski, A.; Rubaszkiewicz, J.; Bednarkiewicz, E. *J. Electroanal. Chem.* **1988**, *239*, 91–105.
(33) Li, C.; Cha, C. *Wulix Huaxne Xuebao* **1988**, *4*, 167; *Chem. Abstr.* *108*, 228364F.
(34) Hill, H. A. O.; Whitford, D. *J. Electroanal. Chem.* **1987**, *235*, 153–167.